Toluene Decompositions over Al-W-incorporated Mesoporous Titanosilicates Photocatalysts

Yeji Lee, Youngmi Kim, Harim Jeong, Min-Kyeong Yeo,† and Misook Kang*

Department of Chemistry, College of Science, Yeungnam University, Gyeongsan, Gyeongbuk 712-749, Korea
**E-mail: mskang@ynu.ac.kr*
†Department of Environmental Science and Engineering, KyungHee University, Yongin, Gyeonggi 449-701, Korea
Received May 22, 2008, Accepted November 14, 2008

This study investigated the decomposition activities of toluene on 10 mol% Al-W-incorporated mesoporous titano (15 mol %) silicates. The mesopore sizes observed in the transmission electron microscopy images ranged from 2.0 to 5.0 nm, and the pores were irregular on the addition of 10 mol% Al or W ions, but changed to regular hexagonal forms with the simultaneous additions of Al and W. The X-ray photon spectroscopy results showed a shift of the special peak for Ti2p in Al-incorporated mesoporous titanosilicates to a stronger binding energy compared to those of mesoporous titanosilicates and Al-incorporated mesoporous titanosilicates. Three O1s peaks in the spectra of the Al and W coexisted samples were observed at 530.5 and 531.7, 533, and 533.7eV, which were assigned to Ti-Os in TiO_2 and Ti_2O_3, Si-O in SiO_2 and Al-O in Al_2O_3, respectively. The toluene molecules desorbed at lower temperatures over W-incorporated mesoporous titanosilicates, and the amounts of toluene desorbed were also small; however, Al-incorporated mesoporous titanosilicates adsorbed much more toluene, particular over $Al_{7.5}$-$W_{2.5}$-Ti_{15}-Si_{75}. The photocatalytic decomposition of toluene was more enhanced over $Al_{7.5}$-$W_{2.5}$-Ti_{15}-Si_{75} than over Al- or W-incorporated mesoporous titanosilicates only.

Key Words: Al-W-incorporated mesoporous titanosilicates, Toluene photodecomposition, Transmission electron microscopy, X-ray photoelectron spectroscopy

Introduction

Mesoporous molecular sieves are used as catalysts and adsorbents in many chemical and petrochemical processes. An understanding of the adsorption and diffusion of molecules within the pores of molecular sieves is important in achieving more efficient uses of and designing new applications for these materials. Hydrocarbon traps, used in many industrial processes,[1-3] is one application of zeolites, where both adsorption and diffusion of molecules play important roles. Many zeolite-catalyst configurations have been proposed. Generally, it has been found that while the heavier exhaust aromatic hydrocarbons (benzene, toluene, and xylene etc) were adequately trapped by zeolites, the light hydrocarbon components of the exhaust stream were often desorbed from the hydrocarbon trap before the catalyst had reached a high enough temperature for combustion to occur. Most recently, semiconductor-loaded zeolites and mesoporous molecular sieves have drawn increasing attention as potential photocatalysts, due to their unique pore structures and adsorption properties.[4-8] Titania has proved to be the most active photocatalytic semiconductor, as it allows complete degradation of pollutants under ultraviolet irradiation. Some researchers have studied the photodegradation of several organic compounds on various TiO_2-loaded zeolites, as well as MCM-41 type molecular sieves. The Ti-loaded mesoporous support in photocatalysis offer: 1) the formation of ultra fine titania particles during sol-gel deposition; 2) increased adsorption, especially for non-polar compounds; 3) higher acidity, which enhances electron abstraction and 4) less UV-light scattering, since silica is the main component of zeolites. The combination of the effects of zeolites and TiO_2 in photocatalytic destruction of aromatic compounds in an aqueous system has been studied. However, the advantage of using a regular structure, such as a zeolite, in gaseous systems has not been clearly identified. In addition, as a loading method for Ti onto the support, impregnation was used in these studies, with very small amounts of loading.

Ti-mesoporous silicates are very useful for the removal of aromatic hydrocarbon molecules, such as benzene toluene, and xylene, as reported in our previous published work. In addition, Al-Ti mesoporous silicates were also been reported to have more super-hydrophilicities than Ti-mesoporous silicate photocatalysts, which resulted in better performance for the removal of volatile organic compounds.[9,10] However, the pore shapes of one metal-incorporated mesoprous titanosilicate were irregular and; in addition, structural damage also occurred as a result of a charge imbalance. Therefore, the adsorption abilities and catalytic performances were not always identical. Finally, the catalytic deactivation also rapidly progressed. Therefore; in this study, attempts were made to incorporate Al or W ions below 10 mol% into mesoporous titano (15 mol %) silicate frameworks to balance the ionic charges and atomic sizes between the metals, which resulted in mesoporous titanosilicates with high structural stability. Consequently, these Al-W-mesoporous titanosilicates ($Al_{7.5}$-$W_{2.5}$-Ti_{15}-Si_{75}, $Al_{5.0}$-$W_{5.0}$-Ti_{15}-Si_{75}, $Al_{2.5}$-$W_{7.5}$-Ti_{15}-Si_{75}, Al_{l0}-Ti_{15}-Si_{75}, W_{10}-Ti_{15}-Si_{75}, and Ti_{25}-Si_{75}) were expected to have high adsorption abilities and photocatalytic decomposition activities for toluene.

Experimental Section

The preparation of Al-W-incorporated mesoporous tita-

nosilicates. Figure 1 shows the general preparation method of Al or W-incorporated mesoporous titanosilicates. The hydrothermal method, which has already been reported in many papers,[4-8] was used in this study. Ludox HS 40 colloidal silica (40 wt-% SiO_2, Dupont), AIP (aluminum triisoproxide, 99.9%, Junsei co.), Tusten hexachloride (99.9%, Junsei co.), and TTIP (titanium tetra-isopropoxide, Junsei co.) were mixed, as the silica, aluminum, tungsten, and titanium sources, respectively, into a solution of sodium hydroxide (NaOH, 99.9%, Aldrich) and distilled water. Cetylmethylammonium bromide (CTMABr, 25 wt-percent, Aldrich) was slowly dropped into the solution to serve as a mesopore template. The composition of the final sol solution was $4.5SiO_2$:1.5-x-yTiO_2:xAl_2O_3:yWO_3:1.0HTACl:1.5Na_2O:0.15$(NH_4)_2O$:350H_2O. The atomic molar ratio of Ti to Si in the gel mixtures was 0.15:0.75, with the other additional metals (Al and W) maintained at 10 mol-percent of the total amounts. The pH was maintained at 11. Crystallization was performed at 100°C for 24 h, and the resulting powder was washed, filtered, and then calcined at 550°C for 6 h in air. Six samples, $Al_{7.5}$-$W_{2.5}$-Ti_{15}-Si_{75}, $Al_{5.0}$-$W_{5.0}$-Ti_{15}-Si_{75}, $Al_{2.5}$-$W_{7.5}$-Ti_{15}-Si_{75}, Al_{l0}-Ti_{15}-Si_{75}, W_{10}-Ti_{15}-Si_{75}, and Ti_{25}-Si_{75}, were designed in this study.

Characterizations of Al-W-incorporated mesoporous titanosilicates. High-resolution transmission electron microscopy (TEM) images of nanometer pore shapes and sizes were obtained on a JEOL 2000EX, with the transmission electron microscope operated at 200 kV. The Brunauer, Emmett and Teller (BET) surface area and pore size distribution (PSD) of the sample were measured *via* nitrogen gas adsorption using a continuous flow method with a chromatograph, equipped with a thermal conductivity detector (TCD), at liquid nitrogen temperature. A mixture of nitrogen and helium was used as the carrier gas, with a GEMINI 2375 model from Micrometrics. The sample was thermally treated at 350°C for 3 h prior to nitrogen adsorption. X-ray photonelectron spectroscopy (XPS) measurements of Ti2p and O1s were recorded on an ESCA 2000 system (VZ Micro-Tech, Oxford, UK), equipped with a non-monochromatic Al*Ka* (1486.6 eV) X-ray source. The Al-W incorporated mesoporous titanosilicate powders were pelletized at 1.2×10^4 kPa for 1 min, and the 1.0-mm pellets then maintained in a vacuum (1.0×10^{-7} Pa) overnight to remove water molecules from the surface prior to measurement. The base pressure of the ESCA system was below 1×10^{-9} Pa. Wide scan spectra were measured over a binding energy range of 0 to 1200 eV, with pass energy of 100.0 eV. Ar^+ bombardment of the catalysts was performed with ion currents between 70 and 100nA. A Shirley function was used to subtract the background from the XPS data analysis. The XPS signals for O1s and Ti2p were fitted using mixed Lorentzian-Gaussian curves. Toluene-temperature programmed desorption (TPD) measurements of the Al-W incorporated mesoporous titanosilicates were carried out on a conventional TPD system, equipped with a TCD cell. The catalysts were exposed to Helium gas, at 550°C for 2 h, to remove the water and impurities from the surface. After pretreatment, the samples were exposed to toluene for 1 h. Finally, programmed heating, at a rate of 10°C/min, was initiated, to a final temperature of 500°C. The quantity of desorbed gas was continuously monitored using the TCD cell. The dehydrated amount and activation energies for H_2O desorption in the Al-W-incorporated mesoporous titanosilicates were determined using thermal gravimeter-differential scattering calorimeter (TG-DSC), equipped with a

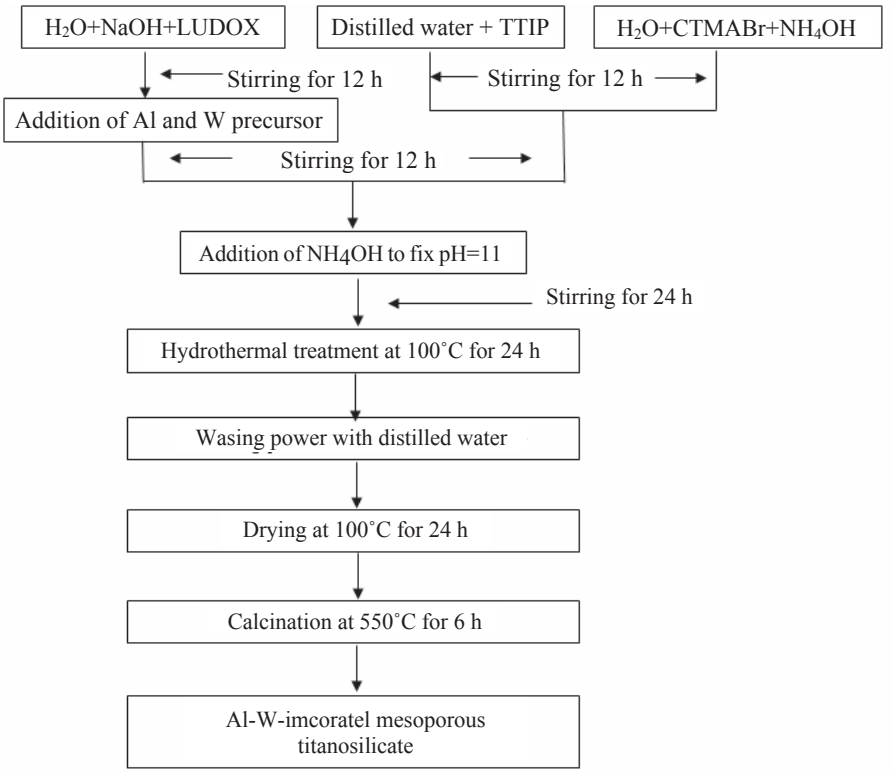

Figure 1. Preparation (hydrothermal method) of the Al-W-incorporated mesoporous titanosilicates.

a) Photos of gas-type reactor for toluene removal

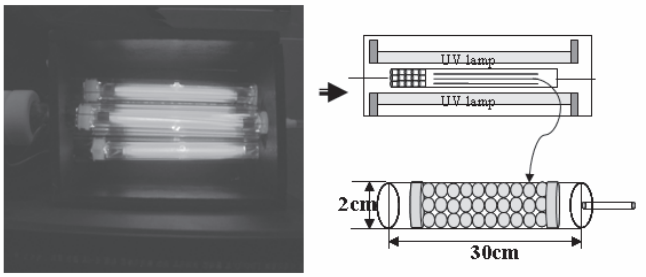

b) Wavelength emitted from UV lamp

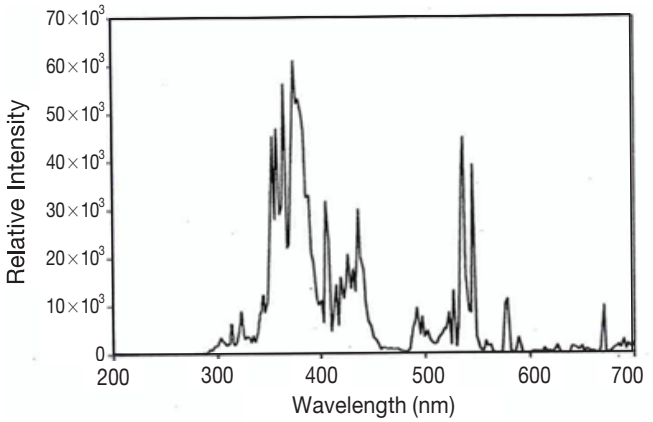

Figure 2. Photoreactor for the decomposition of toluene and the wavelength of the UV-lamps (365 nm). a) Photocatalytic reactor and b) Wavelength of light source

micro thermo-differential and gravimetric analyzer (Perkin Elmer Co., USA). A weight of 20 mg *a*-alumina was used as the reference sample. To maintain identical moisture conditions, the sample was analyzed after being brought into contact with saturated NH_4Cl solution for 24 h.

Analysis of product for toluene decomposition in photocatalytic systems. The decomposition of toluene was carried out using a flow reactor (Figure 2a). A quartz cylinder reactor, 30 cm in length and 2.0 cm in diameter, was used, with ultraviolet(UV)-lamps (model BBL, 365 nm, 24(6×4ea) W/m^2, 20 cm length×1.5 cm diameter, Shinan Co., Korea) used for the photoreaction. The photocatalysts were coated onto 2.0-mm-diameter glass beads as a support, with the quantity of catalyst coating fixed at 1.0 g. The concentration of toluene added to the batch system was fixed at 500ppm. The toluene concentrations before and after photodecomposition were analyzed using gas chromatography. A gas chromatograph (GC), equipped with flame-ionization/thermal-conductivity detectors (FID/TCD) (Shimadzu 17A and HP-5890, respectively) was used to analyze the amounts of toluene and CO_2. To conduct the quantitative gas analysis of the byproducts, *in-situ* Fourier transform infrared (FT–IR) spectroscopy were recorded on a Mattson 1000 spectrometer, using the diffused reflectance method. The powder sample was mixed with CaF_2 and pressed into pellet form. To diminish the influence of H_2O in the air, the pellet was maintained at a temperature of 200°C for 2 h in a dry oven prior to measurement. The scan range was 400 cm^{-1} to 3600 cm^{-1}, with 50 scans accumulated to obtain a resolution

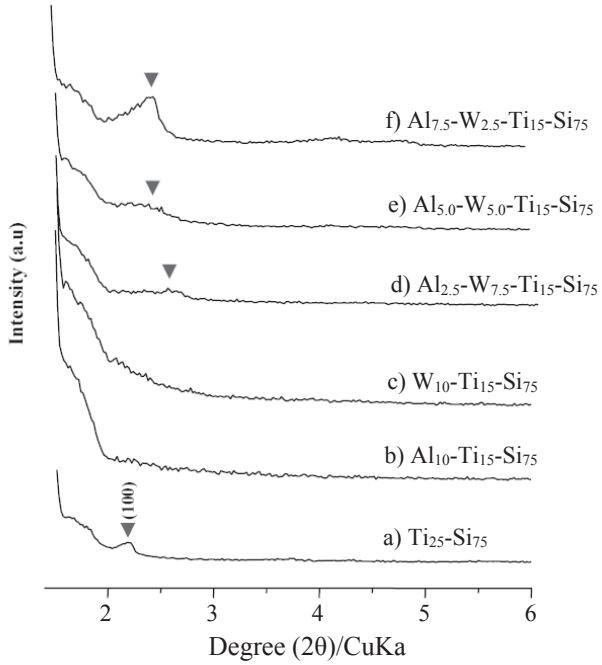

Figure 3. XRD patterns of the synthesized Al-W-incorporated mesoporous titanosilicates.

of 4.0 cm^{-1}. After a steady state had been attained, within 60 min, gas measurements were carried out at 20 min intervals, for 240 min under each set of conditions. For the photodegradation, in a continuous system for the determination of the catalytic lifetime, N_2 gas was used as a carrier gas, with O_2 gas flowed at 40mL/min and a toluene concentration of 100 ppm. All experiments were performed at room temperature and atmospheric pressure. The light radiation of the lamp is shown in Figure 2(b). The main wavelength was distributed in the range 300 to 450 nm.

Results and Discussion

Characterization of Al-W-incorporated mesoporous titanosilicates. Figure 3 shows the X-ray diffraction (XRD) patterns of the Al-W-incorporated mesoporous titanosilicates powders after calcination at 550°C for 6 h. The hexagonal special peaks of pure mesoporous silicate were observed at 100, 110 and 200 planes. However, only (100) plane peaks at 2.25° were shown in all samples, which disappeared on the addition of 10 mol% Al or W ions. This result may be attributable to the collapse of the hexagonal structure due to different atomic sizes. However, the peaks re-appeared, and shifted to a high degree, on the simultaneous additions of Al and W. In general, the peak of (100) plane is known to be shifted to the left when a small amount of titanium is incorporated into a mesoporous silicate with a regular hexagonal structure[12,13]. However, it is of special interest to note that the peak of (100) plane shifted to the right in the Al-W-incorporated mesoporous titanosilicates prepared in this study. In general, when the metals were not incorporated into the framework, the special peaks assigned to titanium or metal oxides were observed after thermal treatment at 550°C. However, no peaks assigned to the added metal oxides were shown in this study, implying the

Table 1. Physical properties of the synthesized Al-W-incorporated mesoporous titanosilicates.

Catalysts	Composition on surface (Atomic %)					Surface Area (cm^2/g)	Pore Volume (cm^3/g)	Pore Size (A^o)
	Al	W	Ti	Si	O			
Ti_{25}-Si_{75}	-	-	4.3.00	14.90	75.20	199.64	0.05	21.04
Al_{10}-Ti_{15}-Si_{75}	0.80	-	7.80	34.50	63.50	138.82	0.02	19.88
W_{10}-Ti_{15}-Si_{75}	0.70	-	5.60	13.20	78.50	251.71	0.13	20.56
$Al_{2.5}$-$W_{7.5}$-Ti_{15}-Si_{75}	0.20	0.70	7.80	18.40	73.10	423.15	0.21	20.28
$Al_{5.0}$-$W_{5.0}$-Ti_{15}-Si_{75}	0.40	0.50	6.40	16.90	79.50	711.26	0.36	20.71
$Al_{7.5}$-$W_{2.5}$-Ti_{15}-Si_{75}	0.60	0.20	5.70	18.60	67.90	811.6	0.41	21.52

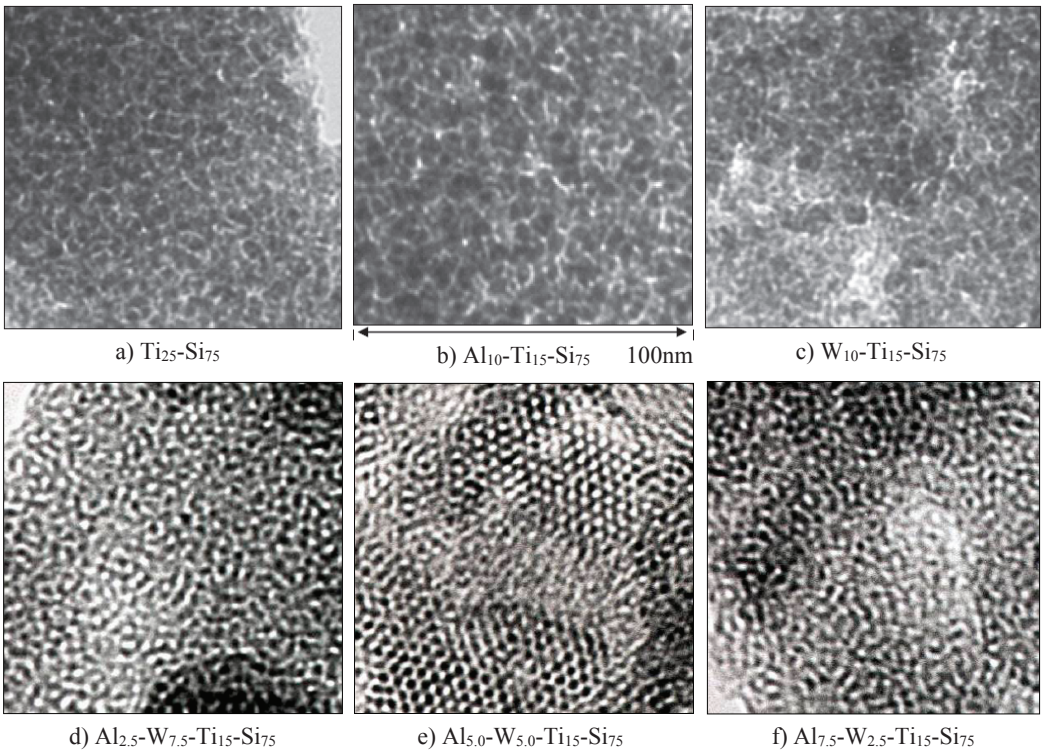

a) Ti_{25}-Si_{75} b) Al_{10}-Ti_{15}-Si_{75} c) W_{10}-Ti_{15}-Si_{75}

d) $Al_{2.5}$-$W_{7.5}$-Ti_{15}-Si_{75} e) $Al_{5.0}$-$W_{5.0}$-Ti_{15}-Si_{75} f) $Al_{7.5}$-$W_{2.5}$-Ti_{15}-Si_{75}

Figure 4. TEM images of the synthesized Al-W-incorporated mesoporous titanosilicates.

metals had been incorporated into the mesoporous titanosilicate framework.

Table 1 summarizes the physical properties of the Al-W-incorporated mesoporous titanosilicates powders. Almost all the real compositions for the Al and W samples, as attained by ICP, were much greater than in the sol solution. The pore volume and diameter were distributed at around 20 angstrom and 0.02-0.41mL/g, respectively. The BET surface areas were below $250cm^2/g$ in Al_{10}-Ti_{15}-Si_{75} and W_{10}-Ti_{15}-Si_{75}, however, these reached 711 to $811cm^2/g$ when Al and W coexisted.

Figure 4 presents the TEM image, showing the detailed pore shapes and sizes in the Al-W-incorporated mesoporous titanosilicates. Diffidently regular hexagonal pores were observed in the pure mesoporous silicate; whereas, the pores in the metal incorporated samples (a, b, c) showed irregular bumpy holes, ranging from 2.0 to 5.0 nm in size. This may be attributable to the difference in the atomic radii between silicon, titanium and the other metals (Al or W), which resulted in variable pore sizes. In particular, with the addition of Al ions into the framework, the pores became more clogged and distorted than that with the addition of W. However, regular pores appeared when Al and W were simultaneously added, with sizes of about 2.5 nm. This result was attributed to the difference in the atomic radii of these ions and the oxidation states of the metals. Consequently, there was a mutual supplement relation between the smaller Al and larger W.

Figure 5 shows typical survey and high-resolution quantitative XPS analyses of the Al-W-incorporated mesoporous titanosilicates. The survey spectra of the metal-mesoporous titanosilicates particles contained both Ti2p and O1s peaks. The $Ti2p_{1/2}$ and $Ti2p_{3/2}$ spin-orbital splitting photoelectrons for all samples were located at binding energies of 464 and 458eV,[14] respectively. In general, a large binding energy implies a higher oxidation state. The curves shifted to larger binding energies on the addition of Al. This result indicates that the Ti oxidation state was changed on the introduction of metal ions. Consequently, this result also implies a change in the Ti-O bonding strength. Generally, the O1s region is divided into several contributions. The main contributions are attributed to Ti-O (530.5eV) in TiO_2, Ti-O (531.7eV) in Ti_2O_3,

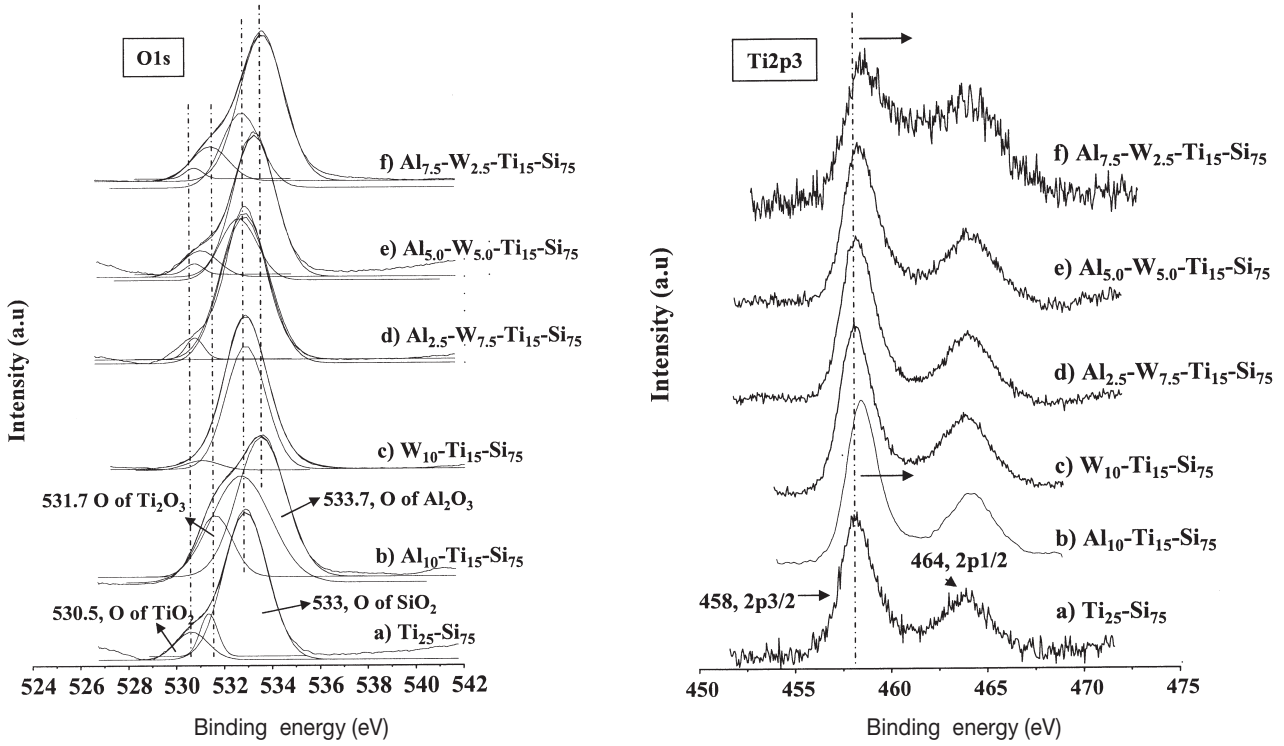

Figure 5. XPS spectra of the synthesized Al-W-incorporated mesoporous titanosilicates.

Si-O (533eV) and Al-O (533.7eV), respectively. Only two spectra assigned to Ti-O inTiO_2 and Si-O in SiO_2 were shown in W10-Ti15-Si75, but four spectra in the Al and W coexisted samples were observed at 530.5, 531.7, 533 and 533.7eV, which were assigned to Ti-O in TiO_2, Ti-O in Ti_2O_3, Si-O in SiO_2 and Al-O in Al_2O_3, respectively, particularly the peak area of Ti-O in Ti_2O_3 was the larger than that of Ti-O in TiO_2. This result proves that the Ti species in the Al-W-incorporated mesoporous titanosilicates were different from the common non-porous or porous titania, which was rather closer to Ti_2O_3 than TiO_2.

Adsorption abilities of toluene and water in Al-W-incorporated mesoporous titanosilicates. Figure 6 shows the TPD curves for toluene desorption from the Al-W-incorporated mesoporous titanosilicates. The adsorbed toluene was desorbed in the range of 50–300℃. The total adsorption abilities for toluene decreased in the order: $Al_{7.5}$-$W_{2.5}$-Ti_{15}-Si_{75}> A_{l0}-Ti_{15}-Si_{75}>W_{10}-Ti_{15}-Si_{75}>Ti_{25}-Si_{75}. These results were attributed to the larger surface area and regular pores in the $Al_{7.5}$-$W_{2.5}$-Ti_{15}-Si_{75}. Conversely, toluene was desorbed at a low temperature from W_{10}-Ti_{15}-Si_{75}; however, the desorption temperature was higher for the Al added samples and the desorbed amount more also increased. This result maybe ascribed to the surface charge effect. On Ti or Si substitutions, the surface was partially negatively charged by the Al^{3+} component, which resulted in toluene being more easily attached to the surface. The adsorbed toluene amount particularly was the best in $Al_{7.5}$-$W_{2.5}$-Ti_{15}-Si_{75} with the higher structural regularity and surface area.

The activation energies for desorptions inform the Al-W-incorporated mesoporous titanosilicates are compared in Table 2. Ozawa presented a useful equation for the calculation

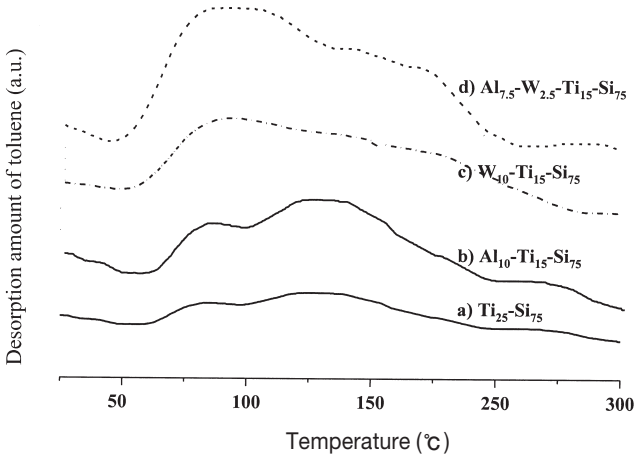

Figure 6. Toluene-TPD of the synthesized Al-W-incorporated mesoporous titanosilicates.

of the activation energy of various thermal reactions, based on the shifts in the maximum deflection temperature, T_m, of the DSC curves on changing the heating rate[11], as follows:

$$\text{Log } \phi + 0.4567E/RTm = \text{constant}$$

Here, ϕ is the heating rate, T_m the maximum deflection temperature, E the activation energy and R the gas constant. The activation energy can be derived from the slope; 0.4567E/R, of a plot of log verse $1/T_m$. This experiment is often used to discuss the hydrophilic property of a structure. Water is known to have a beneficial effect in the photodecomposition of VOC as a donator of OH radicals. Generally, the toluene molecule and water are competitively adsorbed onto the materials'

Table 2. TG curves and activation energy for dehydration in the Al-W-incorporated mesoporous titanosilicates.

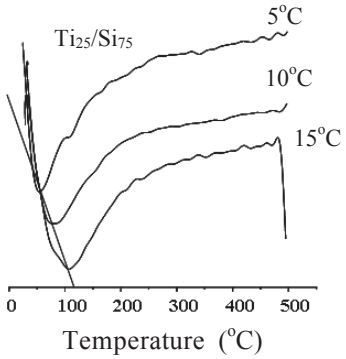

Catalysts	Desorbed H_2O amount (wt%)	Activation energy for H_2O desorption (kcal/mol)
Ti_{25}-Si75	2.50	12.40
Al_{10}-Ti_{15}-Si_{75}	3.75	14.99
W_{10}-Ti_{15}-Si_{75}	2.00	9.10
$Al_{7.5}$-$W_{2.5}$-Ti_{15}-Si_{75}	4.55	15.22

surface. Consequently, if the water desorption activation energy increases, the photocatalytic activity would also increase. In this study, the H_2O desorption energy was the strongest for $Al_{7.5}$-$W_{2.5}$-Ti_{15}-Si_{75} compared with only one metal (Al or W)-incorporated mesoporous titanosilicate photocatalysts. This result implies that $Al_{7.5}$-$W_{2.5}$-Ti_{15}-Si_{75} is more hydrophilic than other mesoporous titanosilicate catalysts.

Toluene photodecomposition on Al-W- incorporated mesoporous titanosilicates. Figure 7 presents the photocatalytic performance of toluene decomposition on the Al-W-incorporated mesoporous titanosilicates. In general, photo-induced adsorption in porous materials is very important, with a fast initial VOC destruction rate, due to their high adsorption properties. When W was incorporated to the framework of the mesoporous titanosilicates, the photodecomposition of toluene occurred slowly, with 150 ppm of toluene destroyed after 240 min. However, the photocatalytic performance markedly increased for the samples incorporated with Al and W, in par ticular, 500 ppm of toluene was completely decomposed over the $Al_{7.5}$-$W_{2.5}$-Ti_{15}-Si_{75}. This result was very remarkable compared to that obtained with non-porous titania photocata lysts. From this result, it can be suggested that the Al-W-incorporated mesoporous titanosilicates are useful for enhancing the removal of macromolecules, such as toluene. Here, the toluene conversion (or photoreaction products) consisted of about 78.0-85.0 wt-% CO_2, 5.0-7.0 wt-% phenol, 10.0-12.0 wt-% benzoic acid, 1.0-3.0 wt-% benzaldehyde, and 1.0 wt-% others, as estimated from the GC-MASS and FT-IR spectra.

At this point, it was realized that the photocatalysis did not go completely to the oxidized forms, i.e. CO_2 and H_2O, but that there were also small amounts of hydrocarbon secondary products. The *in-situ* IR method gives good information for the identification of the secondary products, as shown in Figure 8. Using *in-situ* FT-IR, the peaks for the O-H and C=C double bond of the aromatic compounds, CO_2, vinyl C=C double bonds and O-H were identified. In more detail, the phenol species at 3700 cm^{-1}, alkenes types at 2800 cm^{-1}, and alkynes types at 800 cm^{-1} were observed as secondary products, and CO_2 at 2400 cm^{-1}, H_2O at 3800 cm^{-1} and a benzene residue around 1600-1800 cm^{-1} were also produced. The secon dary by-products were large, and the amount of CO_2 produced from complete photo-oxidation decreased on the addition of W, otherwise the amount of CO_2 increased, and the by-products decreased on the addition of Al. Consequently the

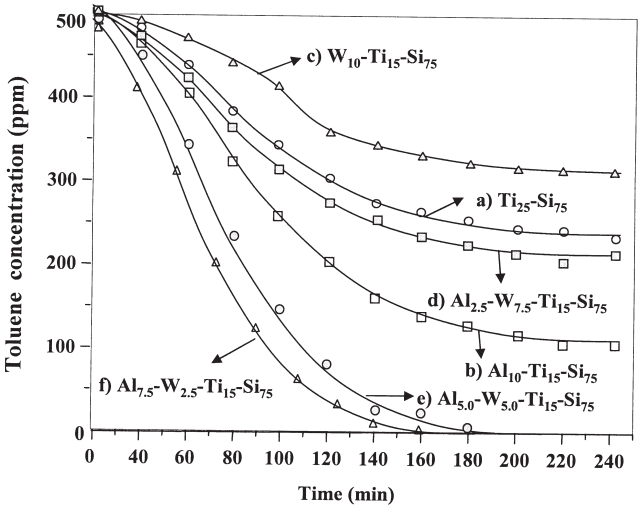

Figure 7. Toluene photodecomposition on the Al-W-incorporated mesoporous titanosilicates. Batch system reaction conditions: Toluene concentration, 500 ppm; Catalyst weight, 1.0g; UV-light intensity, 365 nm; 24 W/m^2

byproducts were particularly well depressed, with the conversion to CO_2 best over $Al_{7.5}$-$W_{2.5}$-Ti_{15}-Si_{75}. This indicates that the Al-W-incorporated mesoporous titanosilicate, with a high surface area and regular pores, was strongly attracted to the toluene molecules, which resulted in a longer retention time of toluene molecules on the surface of the photocatalysts, and consequently, the toluene was easily decomposed.

The photo-catalytic lifetime of $Al_{7.5}$-$W_{2.5}$-Ti_{15}-Si_{75} is shown in Figure 9. Until now, photo-catalytic deactivation has only been discussed in a few reports.[15,16] When 10 vol % H_2O was added during the photocatalytic decomposition of toluene, a toluene conversion of 70% was maintained for 5 days. From this result, the addition of water was assumed to play a role in the generation OH radicals during the photocatalytic reaction. However, without the addition of H_2O, the conversion was slightly decreased after 3.5 days. In addition, the difference between with and without the addition of H_2O was 20%. In this study, if complete toluene photo-catalytic decomposition occurred, then only CO_2 should be produced. However, various by-products, such as phenol, benzoic acid and benzaldehyde, as well as others, have already been confirmed. These products may play a role in the deactivation. However, the by-products formed on the photocatalytic destruction of toluene

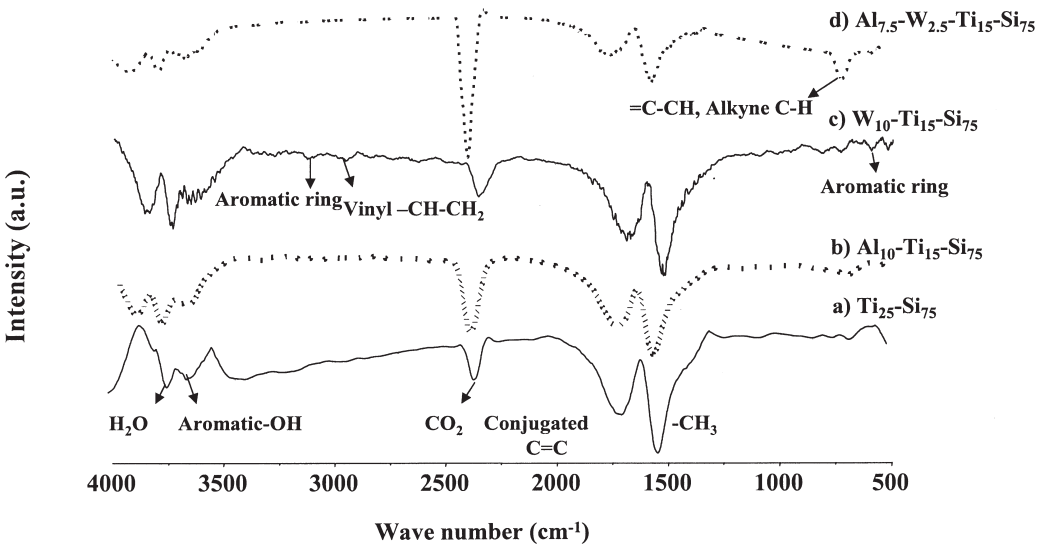

Figure 8. FT-Raman spectra obtained during toluene photodecomposition for 1 h over Al-W-incorporated mesoporous titanosilicates.

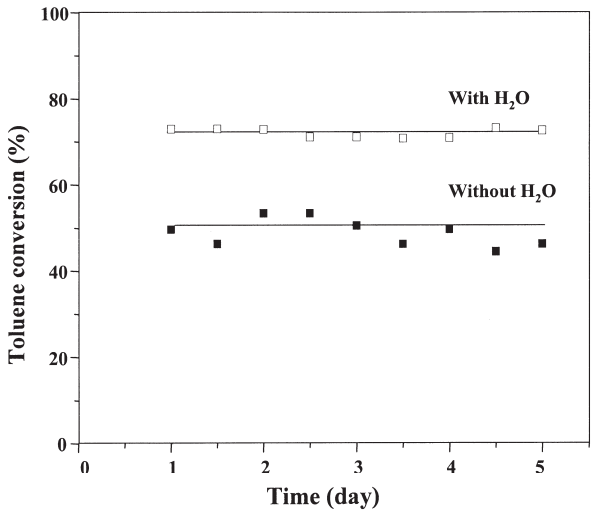

Figure 9. Toluene photodecomposition over $Al_{7.5}$-$W_{2.5}$-Ti_{15}-Si_{75} in the continuous system with or without H_2O. Continuous system reaction conditions: Toluene concentration, 100 ppm; Catalyst weight, 1.0g; UV-light intensity, 365 nm; 24 W/m^2 40 ml/min O_2.

could be depressed by the simultaneous addition of Al and W in the preparation step of the mesoporous titanosilicate and the addition of H_2O during the photocatalytic reaction.

Conclusion

This study investigated the toluene decomposition activities on various Al-W-incorporated mesoporous titanosilicates. The 20-25 angstrom regular hexagonal forms occurred with the coexistence of Al and W ions, with the best surface area obtained for $Al_{7.5}$-$W_{2.5}$-Ti_{15}-Si_{75}. The dehydrated activation energies also increased over the Al-W-incorporated mesoporous titasilicates. The XPS result showed a shift in the special peak for Ti2p in the Al-incorporated mesoporous titanosilicates to a stronger binding energy, and the four O1s types were assigned to Me-O in TiO_2, Ti_2O_3, SiO_2 and Al_2O_3 over the Al-incorporated mesoporous titanosilicates, respectively. The amount of desorbed toluene molecules markedly increased over $Al_{7.5}$-$W_{2.5}$-Ti_{15}-Si_{75}. The photocatalytic decomposition of toluene was greatly enhanced over $Al_{7.5}$-$W_{2.5}$-Ti_{15}-Si_{75} compared to only the Al- or W-incorporated mesoporous titanosilicates, with the high toluene conversion of 70% maintained for 5 days on the addition of H_2O. Consequently, it could be suggested that the mesoporous titanosilicates with the simultaneous incorporations of Al and W are useful for the removal of toluene compared to the individual Al or W-incorporated mesoporous titanosilicates.

Acknowledgments. This research was supported by the Program for the Construction of Eco Industrial Park (EIP) which was conducted by the Korea Industrial Complex Corporation (KICOX) and the Ministry of Knowledge Economy (MKE), for which the authors are very grateful.

References

1. Yang, B. L.; Kung, H. H. *Environ. Sci. Tech.* **1994**, *28*, 1561.
2. Burke, N. R.; Trimm, D. L.; Howe, R. *Stud. Surf. Sci. Catal.* **2000**, *130*, 1451.
3. Czaplewski, K. F.; Reitz, T. L.; Kim, Y. J.; Snurr, R. Q. *Micro. Macro. Mater.* **2002**, *56*, 55.
4. Davydov, L.; Reddy, E. P.; France, P.; Smirniotis, P. G. *J. Catal.* **2001**, *203*, 157.
5. Ikeue, K.; Nozaki, S.; Ogawa, M.; Anpo, M. *Catal. Today* **2002**, *74*, 241.
6. Grieken, R. V.; Aguado, J.; Lopez-Munoz, M. J.; Marugan, J. *J. Photochem. Photobiol A: Chem.* **2002**, *148*, 315.
7. Lee, G. D.; Jung, S. K.; Jeong, Y. J.; Park, J. H.; Lim, K. T.; Ahn, B. H.; Hong, S. S. *Appl. Catal. A: General* **2002**, *6231*, 1.
8. Ahn, W.-S.; Kim, N.-K.; Jeong, S.-Y. *Catal. Today* **2001**, *68*, 83.
9. Kang, M.; Hong, W.-J.; Park, M.-S. *Appl. Catal. B: Environ.* **2004**, *53*, 195.
10. Kang, M.; Lee, M.-H. *Appl. Catal. A: General* **2005**, *284*, 215.
11. Ozawa, T. *J. Therm. Anal.* **1973**, *5*, 563.
12. Koyano, K. A.; Tatsumi, T. *Micro. Mater.* **1997**, *10*, 259.
13. Luo, Y.; Lu, G. Z.; Guo, Y. L.; Wang, Y. S. *Catal. Commun.* **2002**, *3*, 129.
14. Wang, Y.-D.; Ma, C.-L.; Sun, X.-D.; Li, H.-D. *Appl. Catal. A: General* **2003**, *8522*, 1.
15. Kozlov, D. V.; Vorontsov, A. V.; Smirniotis, P. G.; Savinov, E. N. *Appl. Catal. B: Environ.* **2003**, *42*, 77.
16. Lewanandowski, M.; Ollis, D. F. *Appl. Catal. B: Environ*. **2003**, *43*, 309.